3-Dimensional Reconstruction of a Highly Specular or Transparent Cylinder from a Single Image

Arpita Dawda[1](✉), Akash Varasada[2], and Minh Nguyen[1]

[1] Auckland University of Technology, Auckland, New Zealand
arpidawda@gmail.com
[2] Adani Power Mundra Limited, Shiracha, India

Abstract. In production lines, high-speed inspection and quality control are necessary to maintain the quality of a product. Automation in quality checking saves time, reduces manual work, and increases the accuracy of the output. Machine Vision is one of the keys to automation. The inspection of highly specular or transparent surface of the object in ambient lighting conditions is the limitation of traditional machine vision concepts. Some applications do not require to inspect all the features of a product in detail. To overcome time constraints, only essential parameters of the manufactured object are measured during the inspection. For symmetric 3D geometric shape objects, only their perimeter and height are measured. In this paper, a simple approach is proposed to reconstruct the 3-dimensional model of a highly specular or transparent cylinder from a single image captured in a calibrated environment. The paper informs about experiments using the proposed technique; heights and the diameters are measured accurately for three different size cylinders. Two of them are made of stainless steel, and one of them is transparent. All experiments are performed in ambient lighting conditions. The cylinders are translated in X and Y directions with respect to the camera. The dimensions of the cylinders are calculated and compared for five different poses to check the effects of camera position on the accuracy of the results. In the end, the results are compared with the actual dimensions to check the accuracy of the system.

Keywords: 3D reconstruction · Highly specular surface · Transparent object · Metric measurements · Single camera · Single image · Inspection

1 Introduction

In high-speed production lines as seen in Fig. 1, automatic inspection and quality control are necessary to identify faulty and maintain the quality of a product. Machine Vision used to reconstruct 3D information, is one of the keys to

Facteon Intelligent Technology Ltd.

S. Paiva et al. (Eds.): SmartCity360° 2021, LNICST 442, pp. 27–40, 2022.
https://doi.org/10.1007/978-3-031-06371-8_3

such automation. In the last few decades, a significant number of techniques for 3-dimensional (3D) shape measurements have been proposed. These 3D measurement techniques can be classified into two categories: surface contact and surface non-contact techniques [5]. A mechanical probe-based *coordinate measuring machine* (CMM) is one of the examples of surface contact techniques. However, CMM only measures a limited number of points on the surface, and it is relatively slow compared to surface non-contact methods. Also, the surface contact method increases the chances of damage to the object.

For high-speed 3D inspection of objects, surface non-contact techniques are preferred. Time-of-flight, stereo vision, laser range scanning and structured lighting are some of the surface non-contact techniques [2].

Computer stereo vision system uses the same principle by replacing eyes with two CCD or CMOS cameras. They are displaced horizontally to obtain two different views. A disparity map is obtained by finding corresponding points in two slightly different images [22]. The disparity map is used to perform 3D shape measurement.

Among surface non-contact techniques, structured lighting is a widely used 3D shape measurement technique for reflective surfaces. It is used to perform a full-field inspection with high resolution and accuracy. A projector projects a sequence of coded patterns onto object surfaces, and the camera captures images of the reflected pattern. The object surface deforms the reflected patterns. The height information of the object surface is embedded in the phase distribution of the reflected pattern. The calibration is performed to understand the correspondences between the camera and the projector. The 3D coordinates of the object surfaces can be calculated by using phase to height mapping in calibrated environments [2,5]. However, there are many drawbacks of using the above mentioned traditional methods which are explained briefly in next section.

In some applications, it is not essential to reconstruct the detailed 3D model of the object. Only the overall shape of the object and some necessary measurements are sufficient. For example, the diameter and height are the essential

Fig. 1. An automotive stainless steel wheel production line

measurements for a cylindric object. This paper focuses on cylindrical objects. Here, we present a simple approach to reconstruct the overall shape of the highly specular cylinder from a single image captured by a single camera. The same approach could also be applied to calculate the dimensions of other solid shapes such as cubes, cuboids, or prisms. However, one important condition is that the border of the bottom part of the object has to be visible in the image.

The remainder of this paper is structured as follows: Sect. 2 briefly describes all steps of methodology such as calibration of a single camera and ellipse fitting. Section 3 explains all the steps of our technique to measure the height and the diameter of the cylinder in detail. Section 4 shows results for two different cylinders for different poses, compared with actual ground truth. Section 5 concludes.

2 Methodology

Generally, a 3D object is reconstructed using multiple cameras or laser by using the concepts of stereo vision or laser triangulation, respectively [18]. However, both concepts have their own sets of difficulties. To understand the difficulties, we assume that the cylinder is in a vertical position. In stereo vision, two slightly different images of the cylinder are captured in a calibrated environment. Stereo matching is performed on these two images to generate the disparity map [4]. However, it is difficult to find corresponding points for highly specular or transparent objects. The ambient lighting of working environment increases the difficulties for inspection. Also, only the front half of the cylinder would be reconstructed in one go from the disparity map. Moreover, to reconstruct the whole cylinder, we need to rotate the cylinder by 180 °C. The same process of stereo matching is repeated to reconstruct the other half of the cylinder. In the end, both halves are merged. However, it is challenging to merge both halves of the cylinder accurately.

Another option is to use the concept of laser triangulation. Here, a thin luminous straight laser line is projected on to the surface of the cylinder. The camera captures images of the projected line." To reconstruct the whole surface of an object, the object must be moved relative to the measurement system, i.e., the unit built by the laser line projector and the camera [18]." In our case, the cylinder is rotated at regular intervals for reconstruction. However, it is very challenging to calibrate a laser and a camera with respect to a rotating positioning system. If we use a linear positioning system, then we can reconstruct only half of the cylinder in one scan. Therefore, the same problem arises like the one in stereo of merging two halves of the cylinder accurately. Also, if the surface of the cylinder is reflective, the optical signal cannot be correctly retrieved. Therefore, it is usually challenging for any optical method to accurately measure shiny objects or objects with a broad range of reflectivity variation across the surface.

In industrial inspection, we have time constraints which do not allow us to use the expensive process of finding corresponding points such as stereo vision or to do laser triangulation [18]. The flow chart in Fig. 2 represents our suggested approach for the 3D reconstruction of a cylinder using a single camera.

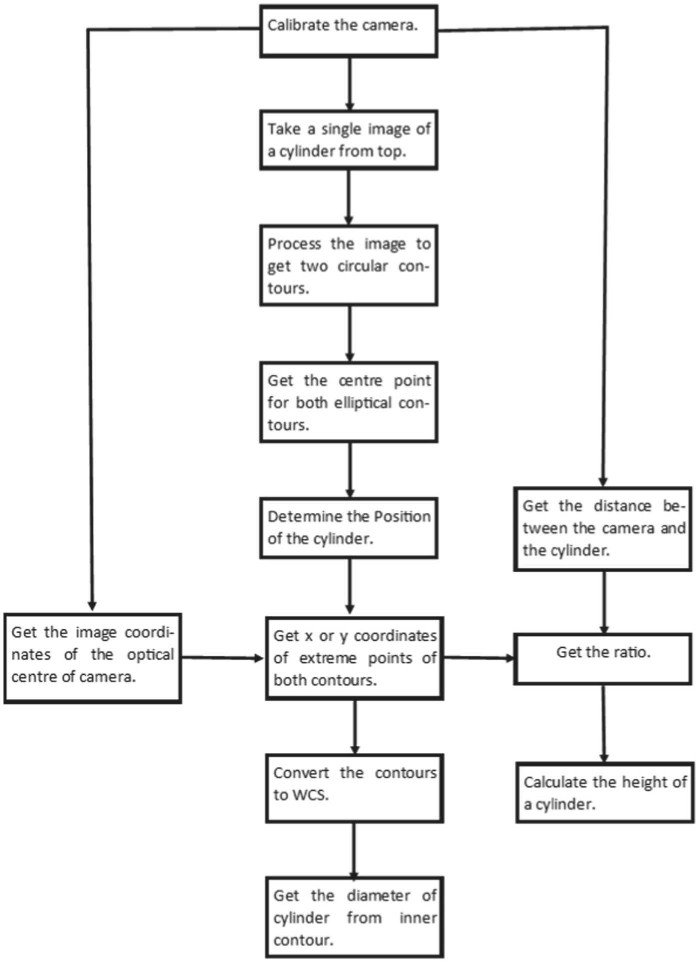

Fig. 2. Overall approach for 3D reconstruction of the cylinder.

2.1 Single Camera Calibration

To perform metric measurements accurately in the world coordinate system (WCS), the only prerequisite is that the camera has been calibrated. The camera is calibrated for a specific plane in WCS for which measurements are obtained. In our case, the calibration plate is placed on besides the cylinder to define the measurement plane. We use calibration plate with hexagonally arranged marks. It contains five finder pattern and atleast one of them should be completely visible in the image for estimating the pose of the relative camera.

Generally, multiple images are captured of a calibration plate in different poses in a specified plane. Here, the specified plane is the measurement plane, which is defined as the plane $Z = 0$ of the WCS. These images, along with the internal camera parameters and the description of calibration plate, work as inputs for calibration. The output comprises the internal and external camera parameters. To determine external parameters, the pose of the calibration plate which is placed directly on the measurement plane is calculated. The external camera parameters describe the relationship between the measurement plane and the camera [18].

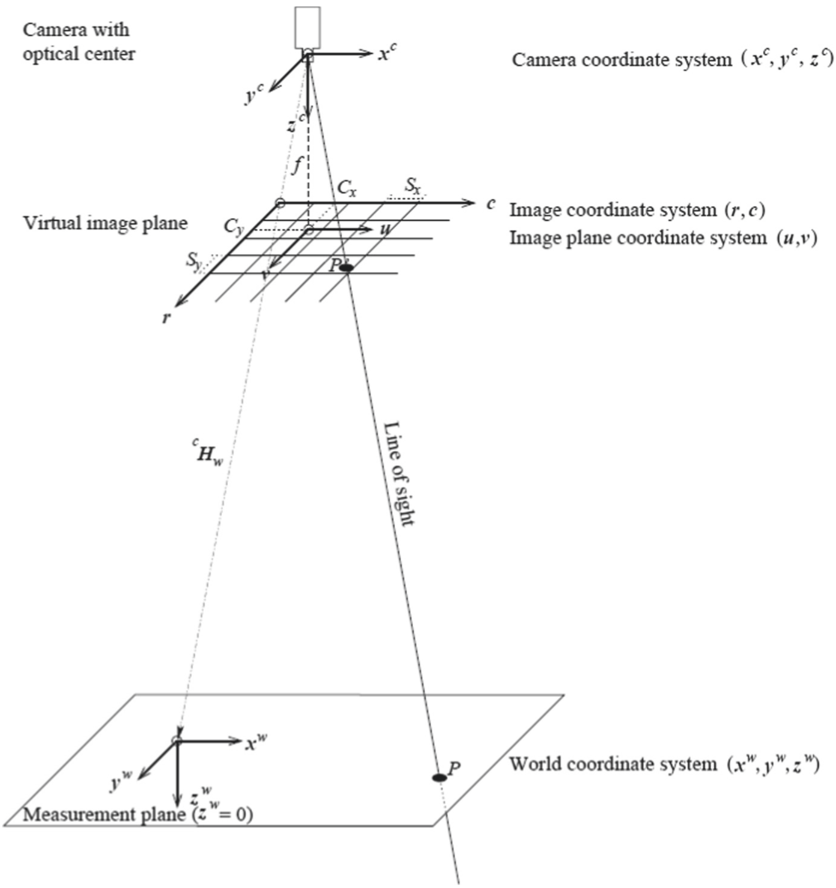

Fig. 3. Transformation of image points in WCS [18].

Figure 3 shows how an image point is transformed into world coordinates. "Given the image coordinates of one point, the goal is to determine the world coordinates of the corresponding point in the measurement plane. For this, the line of sight, i.e., a straight line from the optical centre of the camera through the given point in the image plane, must be intersected with the measurement plane. [18]" The image coordinates are transformed into camera coordinates first and finally into world coordinates using the calibration data.

2.2 Ellipse Fitting

Ellipse extraction is an important task in vision based application as this geometric shape occurs frequently [6,7]. For highly specular or transparent objects, accurate ellipse extraction is difficult. Because low contrast affects accurate extraction of edge contours [8]. "There are three main categories of ellipse extraction methods:Fitting algorithms, Hough-transform techniques, and edge contour following methods [9]." In the first category, an ellipse equation is fitted to a sequence of points. The second category performs ellipse extraction by considering it as a peak-seeking problem in parameter space. Arc-segments are extracted and grouped into an elliptic hypothesis in the last category [9].

In this research, we use Fitting-based edge extraction method as it is proven to be the most accurate among other available methods [10–13]. This method fits an ellipse equation to a sequence of points and tries to minimise the error between the given data and an ellipse equation [14–17]. "There are two types of ellipse-fitting algorithms, algebraic fitting which solves the minimisation problem by exploring the algebraic equation, or geometric fitting which minimises geometric distances of given points to the fitted elliptic curve [9]."

For this research, we use Fitzgibbon's approach for ellipse fitting. This method incorporates the ellipticity constraint into the normalization factor by minimizing the algebric distance. The benefit of using this approach is that it provides useful results under all different noise and occlusion conditions. Also, this direct least-squares fitting method is specifically designed for ellipses. It guarantees that the output will be an ellipse [3].

3 Outline of Our Technique

To reconstruct the cylinder, we need two dimensions, diameter and height of the cylinder. The process of measuring dimensions accurately using a calibrated camera is described below.

3.1 Measurement of the Diameter of a Cylinder

In our approach, the camera is looking at the cylinder from the top instead of the front like conventional 3D reconstruction techniques typically do. After calibrating the camera, a single image of the cylinder is taken from the top. Figure 4 shows an example of the image of the cylinder used for 3D reconstruction. The cylinder shown in image is the largest one among the three cylinders used for this research. This right circular cylinder is made of stainless steel which makes its surface highly reflective. Here, the cylinder is positioned in a way that the bottom and the top of the cylinder is perpendicular to the optical axis of the camera. We can noticeably see two elliptical contours in the image. The camera is calibrated for the bottom plane. Therefore, the edge of the inner ellipse is extracted to measure the diameter of the cylinder. Figure 4 shows the image of the cylinder with detected elliptical contours. It is essential to extract the edges

Fig. 4. An image of the cylinder from top with extracted edges (Courtesy of BLINDED).

of elliptical contours accurately. We need to make sure that the reflection caused by ambient lighting does not affect the accuracy of edge extraction.

Now, we fit an ellipse through the inner contour, which gives us the diameter of the cylinder in the image coordinate system. As stated before, the Fitzgibbon et al. approach is used for ellipse fitting [3]. This extracted inner contour is projected in WCS to get the diameter in metric units. The world coordinates are determined for each point of the detected elliptical contour in the measurement plane. A circular contour will be formed in the measurement plane. We fit a circle through this circular contour using an algebaric approach. This approach minimises the algebraic distance between the contour points and the resulting circle [20]. The diameter of this circular contour in plane $Z = 0$ corresponds to the diameter of the cylinder. The diameter is calculated in metric units using the calibration data.

3.2 Measurement of the Height of a Cylinder

Now, the method to measure the height of the cylinder is described in detail. The setup to measure the height is the same as before. First, the image of the cylinder is processed to accurately extract the edges of two ellipses, which represents the top and the bottom of the cylinder. After extracting the edges, we fit an ellipse through these contours using fitzgibbon approach [19]. Figure 4 shows the image of the cylinder with two extracted edges of elliptical contours. Now, there are three possible cases: (1) The projection centre of the camera and the cylinder's centre line are collinear. (2) The cylinder is horizontally shifted. (3) The cylinder is vertically shifted.

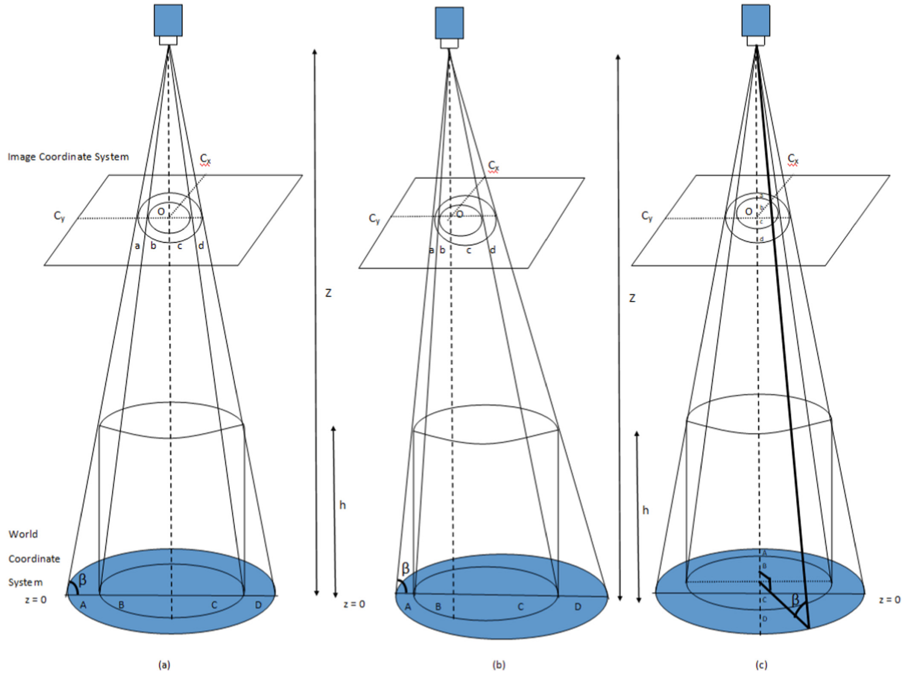

Fig. 5. Three different cases for height measurement.

Figure 5, (a), (b) and (c) illustrate Case 1, Case 2 and Case 3, respectively. As we can see in Fig. 5 (a), we get two concentric elliptical contours in the image plane for Case 1. The second case is shown in Fig. 5 (b). Here, the centre of the camera is not collinear with the centre line of the cylinder. Therefore, we get two elliptical contours which are not concentric. However, the centres of these two elliptical contours share same horizontal axis. Figure 5 (c) shows the third case where the cylinder is vertically displaced. In this case also, the centre of the camera is not collinear with the centre of the cylinder and we get two non-concentric elliptical contours. Instead of horizontal axis, the centres of these two elliptical contours share same vertical axis. Now, our method to measure the height of the cylinder is described in detail below.

To calculate the height, it is essential to find the ratio of $a : b : c : d$ (See Fig. 5). Here, a and d are the distance in pixels between the left extreme points and the right extreme points of both contours, respectively. In case 1 and 2, b and c are the distance between the optical centre and the left and the right extreme points of the internal elliptical contours, respectively. In case 3, b and c are the distance between the optical centre and the top and the bottom extreme points of the internal elliptical contours, respectively. Also, a and d are the distance in pixels between the top extreme points and the bottom extreme points of both contours, respectively. To find this ratio for case 1 and 2, we need to know the X-coordinates of the horizontal extreme points of the contours and also of the optical centre of the camera in the image plane. In case of vertical displacement, we need to know Y- coordinates of the vertical extreme points of the contours and also of the optical centre of the camera in the image plane. The image coordinates of the optical centre of the camera are calculated during the calibration. We can get this parameter by extracting the intrinsic parameters of the camera. After obtaining all the image coordinates the ratio $a : b : c : d$ is calculated. Now, this ratio will correspond to the ratio of $A : B : C : D$ in world coordinate system. A and D represents the height of the cylinder in measurement plane.

We already know that,

$$B + C = D_1 \tag{1}$$

where D_1 is the diameter of the cylinder which is calculated before.

From Fig. 5,

$$A = ax,\ B = bx,\ C = cx,\ D = dx \tag{2}$$

Substituting in Eq. (1),

$$bx + cx = D_1 \tag{3}$$

Here, x is an unknown factor which converts from image coordinate system to world coordinate system:

$$(b + c)x = D_1 \tag{4}$$

$$x = D_1/(b + c) \tag{5}$$

A, B, C and D are calculated by substituting the value of x in Eq. (2). To calculate the height, we also need to know the distance between the camera and the measurement plane. While calibrating the camera, we place the calibration plate directly onto the measurement plane. Therefore, we can determine the distance between the camera and the measurement plane by determining the pose of the calibration plate. The pose of the calibration plate is obtained during the calibration process. By accessing the external parameters of the camera, we can get the distance between the camera and the measurement plane denoted as Z.

Now,

$$\tan\beta = Z/(A + B) = h/A, \tan\beta = Z/(C + D) = h/D \tag{6}$$

In Fig. 5 (c), the angle β is shown slightly to the right for better understanding of the image. In real, the angle β is the angle of the right triangle formed by the camera, the bottom extreme point of outer ellipse and the projection of the centre of the camera in measurement plane.

$$h = (A/(A + B)) \cdot Z, h = (D/(C + D)) \cdot Z \tag{7}$$

Here, h is the height of the cylinder. We can cross-check the results by using the $D/(C + D)$ ratio for height calculation. By measuring the height and the diameter of the cylinder, we can accurately reconstruct the cylinder from a single image.

4 Experiments and Results

Fig. 6. Setup for experiment.

In this experiment, we are using Genie Nano M4020 monochrome camera, which has $4,112 \times 3,008$ resolution. HALCON software is used to perform image processing tasks. The first step of the experiment is to calibrate the camera. The HALCON calibration plate with hexagonally arranged marks is used to calibrate the camera. The calibration plate is placed besides the cylinder (See Fig. 6). This specifies the bottom of the cylinder as the measurement plane. For large objects, we can also place the calibration board inside the cylinder. The camera is mounted at a distance Z from the top of the cylinder. To test this concept, we used three cylinders of different dimensions. Among them, two cylinders are made of stainless steel and one is made of transparent plastic material. Here, a can and a washing machine drum is used to study the case of highly specular surfaces. Figure 7 shows the images of three cylinders used for this research. All experiments are performed in ambient lighting condition of working environment. A single image of the cylinder with the calibration board is captured from the top. The camera is calibrated by using the image of the calibration board as a reference. Now, the cylinder is translated in X and Y directions with respect to the camera. The dimensions of the cylinder are calculated for five different positions.

(a) Transparent Cylinder. (b) Can. (c) Drum.

Fig. 7. Cylinders.

Figure 8 shows the input images of the objects used for this research. Figure 8a shows the case when transparent Cylinder 1 is in leftmost position with respect to the camera. Figure 8b represents the top-most position of Cylinder 2 (a can) with respect to the camera. Figure 8c depicts the collinear axes case for Cylinder 3 (a drum).

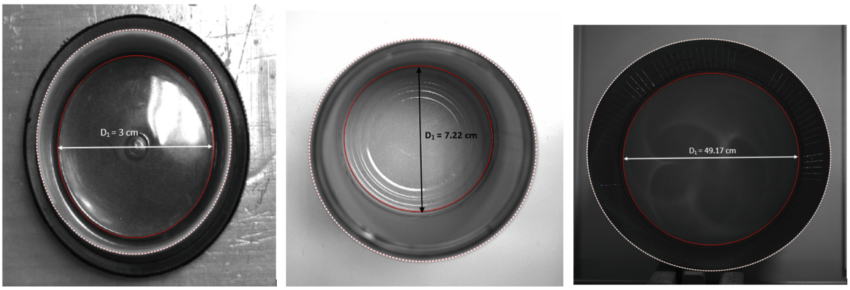

(a) Cylinder 1 in left-most position. (b) Cylinder 2 in top-most position. (c) Cylinder 3 in centre position.

Fig. 8. Cylinders with extracted elliptical contours.

The edges of the two elliptical contours are extracted by applying thresholding and edge detection algorithms. After extracting the edges, fitzgibbon approach is applied to fit an ellipse through these contours [19]. The image coordinates of the extreme points of the two elliptical contours are obtained from elliptical contours. Also, the projection of the optical centre of the camera in the image coordinate system is obtained as a result of calibration. The diameter of the inner ellipse in the world coordinate system depicts the diameter of the cylinder. In Fig. 8, the diameter of all three cylinders for the given case are mentioned.

Now, the distance between the camera and the measurement plane and the image coordinates of the optical centre of the camera are two crucial parameters for height calculation. Both of them are obtained as a result of calibration. Here, the distance between the camera and the measurement plane is 35.194 cm for Cylinder 1 and 2 and 106.062 cm for Cylinder 3.

Now, the height of the cylinder is measured using the method defined above. Table 1 compares the results for five different positions of the cylinders in either X or Y direction with the actual parameters for Cylinder 1, 2 and 3. The accuracy of the output is also calculated in the table. Moreover, the accuracy of the output predominantly depends on the accuracy of the calibration. Another critical factor is the edge detection and ellipse fitting step for the two elliptical contours.

Table 1. Comparison of output dimensions.

Objects	Cylinder 1			Cylinder 2			Cylinder 3		
Dimensions	Height (cm)	Diameter (cm)	Accuracy (%)	Height (cm)	Diameter (cm)	Accuracy (%)	Height (cm)	Diameter (cm)	Accuracy (%)
Actual Dimensions	3	3	-	12.5	7.3	-	37	49.5	-
Left-most Position	2.79	2.8	94	11.58	7.22	94.94	36.71	49.26	99.39
Right-most Position	2.87	3	97.83	12.38	7.21	98.93	36.85	48.98	99.22
Centre Position	2.89	3	98.16	12.43	7.22	99.24	36.92	49.17	99.53
Top-most Position	2.69	2.9	96.83	12.49	7.22	99.54	35.74	48.79	97.72
Bottom-most Position	2.75	2.9	95.5	12.37	7.22	98.93	36.98	49.24	99.67

5 Conclusion

To conclude, this research provides a simple, fast, cost-effective and feasible approach for the 3D reconstruction of even a highly specular or transparent cylinder from a single image. The main advantage of this method is that it overcomes the limitation of traditional machine vision methods and solves the problem of inspecting highly specular or transparent objects even in ambient lighting conditions. To do so, the only prerequisite is that the top and the bottom of the cylinder are perpendicular to the optical axes of the camera. Also, it is necessary that we can accurately extract the two elliptical contours which represent the top and the bottom of the cylinder. Another crucial parameter of this research is the calibration of the camera as all important parameters required for measurements are obtained from the output of the calibration. The accuracy of output is inversely proportional to the calibration error. For small calibration error, we can achieve the highest accuracy. By analysing the results, the accuracy of the output does not depend on the position of the cylinder with respect to the camera or on the size of the cylinder.

Moreover, this research could also be used for calculating the dimensions of other types of solid shapes such as cube, cuboids or prisms. Also, we can calculate the volume and the surface area of the product from measured dimensions. Due to the time efficiency of the designed solution, the method is applicable in the industrial production and inspection process.

Acknowledgement. Supported by Facteon Intelligent Technology Ltd.

References

1. Asoudegi, E., Pan, Z.: Computer vision for quality control in automated manufacturing systems. Comput. Ind. Eng. **21**(1–4), 141–145 (1991)
2. Chen, F., Brown, G., Song, M.: Overview of three-dimensional shape measurement using optical methods. Opt. Eng. **39**(1), 10–22 (2000)
3. Fitzgibbon, A., Pilu, M., Fisher, R.B.: Direct least square fitting of ellipses. IEEE Trans. Pattern Anal. Mach. Intell. **21**(5), 476–480 (1999)
4. Klette, R.: Concise Computer Vision. Springer, London (2014). https://doi.org/10.1007/978-1-4471-6320-6
5. Lin, H., Gao, J., Zhang, G., Chen, X., He, Y., Liu, Y.: Review and comparison of high-dynamic range three-dimensional shape measurement techniques. J. Sensors (2017)
6. Pătrăucean, V., Gurdjos, P., Gioi, V.: Joint a contrario ellipse and line detection. IEEE Trans. Pattern Anal. Mach. Intell. **39**, 788–802 (2017)
7. Ren, J., Owais, H.M., Song, T., Lin, D.: Towards fast and accurate ellipse and semi-ellipse detection. In: Proceedings of IEEE International Conference on Image Processing, pp. 743–747 (2018)
8. Ouellet, J.N., H'ebert, P.: Precise ellipse estimation without contour point extraction. Mach. Vis. Appl. **21**, 59–67 (2010)
9. Xu, Z., Xu, S., Qian, C., Klette, R.: Ellipse extraction in low-quality images. In: 2019 16th International Conference on Machine Vision Applications (MVA), pp. 1–5. IEEE (2019)
10. Kanatani, K., Sugaya, Y., Kanazawa, Y.: Ellipse fitting. In: Guide to 3D Vision Computation, pp. 11–32 (2016)
11. Kanatani, K., Sugaya, Y., Kanazawa, Y.: Ellipse Fitting for Computer Vision: Implementation and Applications. Morgan and Claypool, Williston (2016)
12. Kovalevsky, V.: Modern Algorithms for Image Processing. Apress, Springer, Delware (2019). https://doi.org/10.1007/978-1-4842-4237-7
13. Masuzaki, T., Sugaya, Y., Kanatani, K.: High accuracy ellipse-specific fitting. In: Klette, R., Rivera, M., Satoh, S. (eds.) PSIVT 2013. LNCS, vol. 8333, pp. 314–324. Springer, Heidelberg (2014). https://doi.org/10.1007/978-3-642-53842-1_27
14. Prasad, D.K., Leung, M.K., Quek, C.: ElliFit: an unconstrained, noniterative, least squares based geometric ellipse fitting method. Pattern Recogn. **46**, 1449–1465 (2013)
15. Wang, Y., He, Z., Liu, X., Tang, Z., Li, L.: A fast and robust ellipse detector based on top-down least-square fitting. In: Proceedings of British Machine Vision Conference, pp. 156.1–156.12 (2015)
16. Mulleti, S., Seelamantula, C.S.: Ellipse fitting using the finite rate of innovation sampling principle. IEEE Trans. Image Process. **25**, 1451–1464 (2016)

17. Chojnacki, W., Brooks, M.J., Hengel, A.V.D., Gawley, D.: On the fitting of surfaces to data with covariances. IEEE Trans. Pattern Anal. Mach. Intell. **22**, 1294–1303 (2000)
18. Solution Guide III-C 3D Vision, Machine Vision in 3D World Coordinates, Version 18.05, MVTec Software GmbH, München (2018)

Websites

19. fit_ellipse_contour_xld (2019). www.mvtec.com/doc/halcon/12/en/fit_ellipse_contour_xld.html
20. fit_circle_contour_xld (2019). www.mvtec.com/doc/halcon/12/en/fit_circle_contour_xld.html
21. Machine Vision 2019. https://en.wikipedia.org/wiki/Machine_vision. Accessed 10 July 2019
22. Stereo Vision 2017, The MathWorks Inc. http://au.mathworks.com/discovery/stereo-vision.html. Accessed 13 July 2019